The multi-level Dicke model in ultracold gases

Bachelor Thesis

by

Maximilian Bucher

born on the 4th of January 1988 in Frankfurt am Main

March 31, 2011

Supervisors:
Prof. Dr. Tobias Brandes
Dr. Clive Emary

Institut für Theoretische Physik
Hardenbergstr. 36
TU Berlin
D-10623 Berlin
Germany

Abstract

This thesis develops a multi-mode expansion of the Dicke model. The mode expansion itself is induced by a full set of Bloch functions. A generalized Holstein-Primakoff transformation, displacement operators and the thermodynamic limit lead to a effective model.

An exact effective multi-mode model of the normal phase is shown and the Dicke-type phase transition is pointed out. The complicated system in the super-radiant phase had to be treated numerically, but the behavior of the Bose-Einstein condensate mode population as well as the behavior of the cavity mode is shown.

Die selbständige und eigenhändige Anfertigung versichert an Eides statt
Berlin, den 31. März 2011

Maximilian Bucher

Contents

1 Introduction

Ultra cold bosonic gases (BEC) in a high-finesse optical cavity undergo a phase transition, which can be controlled by tuning the intensity of a laser. In the normal phase is no photon in the cavity,

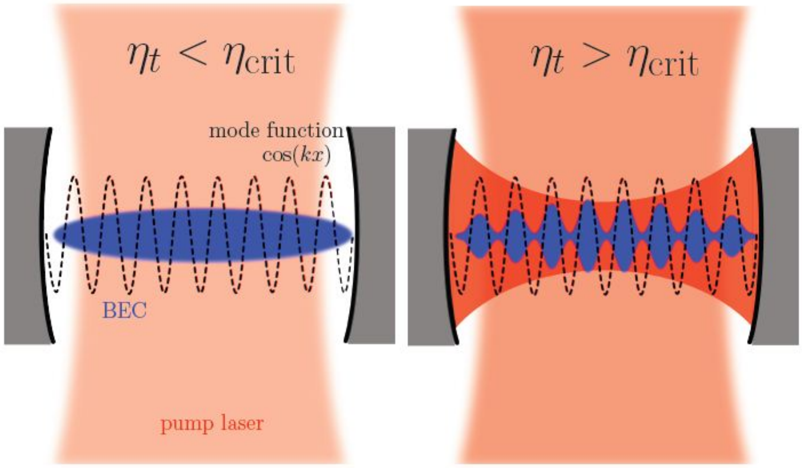

Figure 1: The pump power η_t leads to a phase transition. Below the critical value η_{crit} we can see the normal phase (left) with a quasi-homogenious cloud and above this critical value we see the super-radiant phase and the self-organization of a Bose-Einstein condensate (right). In the super-radiant phase it is also illustrated, that there are photons in the cavity. Graphics by [6]

while in the super-radiant phase photons can be observed. In the normal phase the ultra cold gases create a homogeneous cloud, whereas in the super-radiant phase the BEC self-organizes due to the scattered pump light. This self-organization was experimentally shown recently by [2], who have shown the analogy to the Dicke model phase transition as well. Often, the normal Dicke-type phase transition is discussed with a fixed number of atoms and a two mode Hilbert space [4, 7]. In that case it is necessary to introduce a Holstein-Primakoff spin representation. However, the method using a Holstein-Primakoff transformation did not only show the normal Dicke-type phase transition, it also showed the phase transition in the 1D, two-level Dicke model by [7].

In this thesis I will expand the Dicke model to a multi-mode model. It is then possible to give a more detailed description of the normal phase, a better understanding of the phase transition and the super-radiant phase.

The thesis is organized as follows. The introduction to the microscopic 1D model and the field operators can be found in section 1.1. The multi-mode Hamiltonian in second quantization is derived in section 1.2 and is followed by the generalized Holstein-Primakoff mapped Hamiltonian in chapter 2. It is then required to use displacement operators and to make use of the thermodynamic limit as done in chapter 3. We can then derive solutions for the displacement factors, which lead to the effective Hamiltonians for the normal phase and the super-radiant phase, as shown in chapter 4.

1.1 Microscopic model

We consider a Bose-Einstein condensate, which is trapped in a high-Q optical cavity, that has a single mode of frequency ω_C. The total number of atoms is N and the BEC is interacting with only this single cavity mode. The ultra cold gas is coherently driven from the side by a laser pump field of a frequency ω, which is far below atomic resonance frequency ω_A. The atom-pump detuning

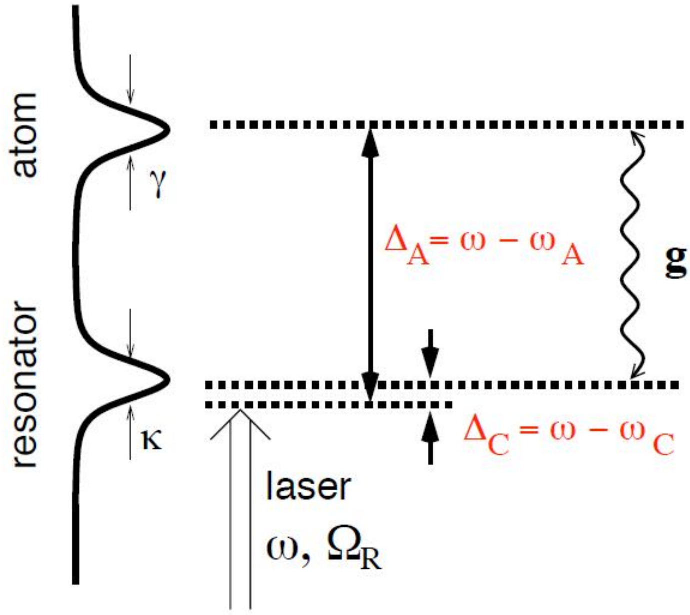

Figure 2: The illustration of the system and it's parameters. κ and γ are linewidths. Graphic by [6]

$\Delta_A = \omega - \omega_A < 0$ leads to a low electronic excitation in the atoms, so the photon emission from the atoms is suppressed. Also the laser is almost resonant to the cavity mode, so the photon scattering is also a nearly resonant process. Due to the typically short length of the cavity there is a strong dipole coupling between the resonator mode and the BEC, its characterization is the single-photon Rabi frequency g_0. The strength of the dispersive atom-field interaction is $U_0 = \frac{g_0^2}{\Delta_A}$. For simplicity, we describe the cavity along the x-axis, where the cavity mode function is $cos(k_0 x)$. The total length of the cavity is Lp, while $L = \frac{\lambda}{2}$ and p is the quantity of the L-modes. The corresponding wavenumber is $k_0 = \frac{2\pi}{L}$. The many-particle Hamilton operator with $\hbar = 1$ reads

$$H = -\Delta_C a^\dagger a + \int_0^{Lp} \hat{\Psi}^\dagger(x) \left[-\frac{1}{2m} \frac{d^2}{dx^2} + U_0 a^\dagger a cos^2(k_0 x) + \eta_t cos(k_0 x) \left\{ a^\dagger + a \right\} \right] \hat{\Psi}(x) dx, \quad (1.1)$$

where $\hat{\Psi}(x)$ is the annihilation operator of the atom field and a the annihilation operator of the cavity mode. The detuning $\Delta_C = \omega - \omega_C$ is the effective photon energy in the cavity. Besides the dispersive atom-field interaction term $U_0 cos^2(k_0 x)$ is $\eta_t cos(k_0 x)$ describing the effective cavity pump with the amplitude $\eta_t = \frac{\Omega g_0}{\Delta_A}$, where Ω is the Rabi frequency.
To summarize, we have a mix of four waves: The cavity mode, the condensate and the dispersive interaction terms.

1.2 Multi-level expansion

As discussed in reference [8] Bloch functions are a good option for a full set of single-particle wave functions. In general this is also described in reference [1]. Here, the field-operators are introduced as

$$\hat{\Psi}(x) = \frac{1}{\sqrt{Lp}} \sum_{n=-\infty}^{\infty} b_n e^{\mathrm{i}(nk_0+q)x}, \tag{1.2}$$

where $\frac{1}{\sqrt{Lp}}$ is the normalization factor, b_n are bosonic annihilation operators and for p even,

$$n = 0, \pm 1, \pm 2, \dots; \quad q = \frac{2\pi}{Lp} m \;\text{ with }\; m = -\frac{p}{2}+1, -\frac{p}{2}+2, \dots, \frac{p}{2}-1, \frac{p}{2}.$$

We may identify q as the quasi-impulse, which is important for describing gases, that have a interaction involving this impulse.

We are now interested in how the Hamiltonian (1.1) looks like in this n-level subspace spanned by (1.2) and its complex conjugate. In this step we move on to second quantization which may be written as

$$\sum_{n,n',q,q'}^{\infty} \int_0^{Lp} dx \hat{\Psi}^{\dagger}_{n',q'}(x) \underbrace{\left[-\frac{1}{2m}\frac{d^2}{dx^2} + U_0 a^{\dagger} a cos^2(k_0 x) + \eta_t cos(k_0 x)\left\{ a^{\dagger} + a \right\} \right]}_{\hat{h}(x)} \hat{\Psi}_{n,q}(x) \tag{1.3}$$

$$= \underbrace{\sum_{j}^{P}}_{p} \sum_{n,n',q,q'}^{\infty} \frac{1}{Lp} \int_0^L dx b^{\dagger}_{n',q'} e^{-\mathrm{i}(nk_0+q)x} \hat{h}(x) b_{n,q} e^{\mathrm{i}(nk_0+q)x} \tag{1.4}$$

$$\begin{aligned} = \sum_{n,n',q,q'}^{\infty} \frac{1}{L} \int_0^L dx \Bigg\{ & (nk_0+q)^2 \underbrace{e^{\mathrm{i}k_0(n-n')x}}_{\delta_{n,n'}} \underbrace{e^{\mathrm{i}k_0(q-q')x}}_{\delta_{q,q'}} b^{\dagger}_{n',q'} b_{n,q} \\ & + \frac{U_0}{4}\delta_{q,q'} \Bigg(\underbrace{e^{\mathrm{i}k_0(n-n'+2)x}}_{\delta_{n+2,n'}} + 2 + \underbrace{e^{\mathrm{i}k_0(n-n'-2)x}}_{\delta_{n,n'+2}} \Bigg) b^{\dagger}_{n',q'} b_{n,q} a^{\dagger} a \\ & + \delta_{q',q} \Bigg(\underbrace{e^{\mathrm{i}k_0(n-n'+1)x}}_{\delta_{n+1,n'}} + \underbrace{e^{\mathrm{i}k_0(n-n'-1)x}}_{\delta_{n,n'+1}} \Bigg) b^{\dagger}_{n',q'} b_{n,q} \left(a^{\dagger} + a \right) \Bigg\}. \end{aligned} \tag{1.5}$$

The Hamiltonian evolves to

$$\begin{aligned} H = -\Delta_C a^{\dagger} a + \sum_{q=-\frac{p}{2}+1}^{\frac{p}{2}} \sum_{n=-\infty}^{\infty} \frac{1}{2} \left[(nk_0+q)^2 + U_0 a^{\dagger} a \right] b^{\dagger}_n b_n \\ + \frac{1}{4} U_0 a^{\dagger} a \left[b^{\dagger}_{n+2} b_n + b^{\dagger}_n b_{n+2} \right] + \frac{1}{2}\eta (a^{\dagger} + a) \left[b^{\dagger}_{n+1} b_n + b^{\dagger}_n b_{n+1} \right]. \end{aligned} \tag{1.6}$$

The Hamiltonian (1.6) provides a good image of the interaction between the modes. As already expected the interaction between the modes b_n, b_{n+1} is similar to the two-level Dicke model. It is also easy to see, that there is an interesting new interaction between the modes b_n, b_{n+2} generated by the mode function $\cos^2(k_0 x)$. We may also identify the kinetic energy term of the condensate

and the unchanged cavity mode.
The quasi-impulse q is not involved in any interactions between the modes. Due to the zero-temperature BEC, which starts at $q = 0$ and because there are no interactions, the BEC does not leave the $q = 0$ sector, so that we may neglect it in the following thesis.

1.3 Multi-level expansion with trigonometric functions

From a symmetry point-of-view it might be better to work with cos- and sin-functions rather than exponentials. Beginning with (1.2), we can write

$$\hat{\Psi}(x) = \frac{1}{\sqrt{Lp}} \sum_{n=-\infty}^{\infty} b_n \left[cos(nk_0x) + \mathrm{i} sin(nk_0x)\right]. \tag{1.7}$$

Due to the symmetry of the trigonometric functions and because we want to get rid of as many terms as possible, the field-operator transforms to

$$\hat{\Psi}(x) = \frac{1}{\sqrt{Lp}} \left[\underbrace{b_0}_{\hat{c}_0} + \frac{1}{\sqrt{Lp}} \sum_{n=1}^{\infty} \underbrace{\left(\frac{b_n + b_{-n}}{A}\right)}_{\hat{c}_n} cos(nk_0x) + \sum_{n=1}^{\infty} \mathrm{i} \underbrace{\left(\frac{b_n - b_{-n}}{A}\right)}_{\hat{s}_n} sin(nk_0x) \right], \tag{1.8}$$

$$\hat{\Psi}(x) = \frac{1}{Lp}\hat{c}_0 + \frac{1}{\sqrt{Lp}} \sum_{n=1}^{\infty} \left[\hat{c}_n cos(nk_0x) + \mathrm{i}\hat{s}_n sin(nk_0x)\right], \tag{1.9}$$

where $\hat{c}_n$, $\hat{s}_n$ have to fulfill the bosonic commutation relations, so we can derive the normalization factor A by solving the commutator:

$$\left[\hat{c}_n, c_m^\dagger\right] = \delta_{nm} \qquad \text{for n=m,} \tag{1.10a}$$

$$\left[\frac{b_n + b_{-n}}{A}, \frac{b_n^\dagger + b_{-n}^\dagger}{A}\right] = 1 \tag{1.10b}$$

$$\frac{1}{A^2}\left(\underbrace{\left[b_n, b_n^\dagger\right]}_{1} + \underbrace{\left[b_{-n}, b_{-n}^\dagger\right]}_{1}\right) = 1 \tag{1.10c}$$

$$A = \sqrt{2} \tag{1.10d}$$

The new operators $\hat{c}_0$, $\hat{c}_n$ and $\hat{s}_n$ are given by

$$\hat{c}_0 = b_0, \tag{1.11a}$$

$$\hat{c}_n = \frac{b_n + b_{-n}}{\sqrt{2}}, \tag{1.11b}$$

$$\hat{s}_n = \frac{b_n - b_{-n}}{\sqrt{2}} \tag{1.11c}$$

and we might therefore prefer to write

$$\hat{\Psi}(x) = \frac{1}{\sqrt{Lp}} \left\{ \hat{c}_0 + \sqrt{2} \sum_{n>0}^{\infty} \hat{c}_n \cos(nk_0 x) + \sqrt{2} \sum_{n>0}^{\infty} \hat{s}_n \sin(nk_0 x) \right\}. \tag{1.12}$$

In order to skip the step where we would have to evaluate the field operator in the Hamiltonian, like in section 1.2, we may use the Hamiltonian (1.6) and replace the b_n, b_{-n} operators with

$$b_0 = \hat{c}_0, \tag{1.13a}$$

$$b_n = \frac{\hat{c}_n + \hat{s}_n}{\sqrt{2}}, \tag{1.13b}$$

$$b_{-n} = \frac{\hat{c}_n - \hat{s}_n}{\sqrt{2}}. \tag{1.13c}$$

In order to gain insight into transforming the Hamiltonian, it is shown by one of the dispersive atom-interaction terms.

$$\begin{aligned} H^{(3)} = \frac{1}{2}\eta_t \left(a^\dagger + a\right) \Bigg[& \overbrace{b_1^\dagger b_0 + b_0^\dagger b_1}^{n=0} + \overbrace{b_{-1}^\dagger b_0 + b_0^\dagger b_{-1}}^{n=-1} \\ & + \sum_{n\geq 1}^{\infty} \left(b_{n+1}^\dagger b_n + b_n^\dagger b_{n+1} \right) + \sum_{n\geq 2}^{\infty} \left(b_{-n}^\dagger b_{-(n-1)} + b_{-(n-1)}^\dagger b_{-n} \right) \Bigg] \end{aligned} \tag{1.14}$$

$$\begin{aligned} H^{(3)} = & \frac{1}{2}\eta_t \left(a^\dagger + a\right) \\ & \Bigg[\frac{1}{\sqrt{2}} \left\{ \left(\hat{c}_1^\dagger + \hat{s}_1^\dagger\right) \hat{c}_0 + \hat{c}_0^\dagger \left(\hat{c}_1 - \hat{s}_1\right) + \hat{c}_0^\dagger \left(\hat{c}_1 + \hat{s}_1\right) + \left(\hat{c}_1^\dagger - \hat{s}_1^\dagger\right) \hat{c}_0 \right\} \\ & + \frac{1}{2} \Bigg\{ \sum_{n\geq 1}^{\infty} \left(\hat{c}_{n+1}^\dagger + \hat{s}_{n+1}^\dagger\right) \left(\hat{c}_n + \hat{s}_n\right) + \left(\hat{c}_n^\dagger + \hat{s}_n^\dagger\right) \left(\hat{c}_{n+1} + \hat{s}_{n+1}\right) \\ & + \underbrace{\sum_{n\geq 2}^{\infty} \left(\hat{c}_{n-1}^\dagger - \hat{s}_{n-1}^\dagger\right) \left(\hat{c}_n - \hat{s}_n\right)}_{I} + \left(\hat{c}_n^\dagger - \hat{s}_n^\dagger\right) \left(\hat{c}_{n-1} - \hat{s}_{n-1}\right) \Bigg\} \Bigg] \end{aligned} \tag{1.15}$$

For simplicity we can write the term I as

$$I = \sum_{n\geq 2}^{\infty} \left(\hat{c}_{n-1}^\dagger - \hat{s}_{n-1}^\dagger\right) \left(\hat{c}_n - \hat{s}_n\right), \qquad \text{with } k = n-1 \tag{1.16a}$$

$$= \sum_{k\geq 1}^{\infty} \left(\hat{c}_k^\dagger - \hat{s}_k^\dagger\right) \left(\hat{c}_{k+1} - \hat{s}_{k+1}\right) \tag{1.16b}$$

$$= \sum_{n\geq 1}^{\infty} \left(\hat{c}_n^\dagger - \hat{s}_n^\dagger\right) \left(\hat{c}_{n+1} - \hat{s}_{n+1}\right) \tag{1.16c}$$

Now the full hamiltonian (1.6) in $\hat{c}$-algebra may be written as

$$\begin{aligned} H =& -\Delta_C a^\dagger a + \frac{1}{4}U_0 a^\dagger a \left(2\hat{c}_0^\dagger \hat{c}_0 + \hat{c}_1^\dagger \hat{c}_1 - \hat{s}_1^\dagger \hat{s}_1\right) + \frac{1}{2}\sum_{n\geq 1}^{\infty}\left\{\left(n^2 k_0^2 + U_0 a^\dagger a\right)\left(\hat{c}_n^\dagger \hat{c}_n + \hat{s}_n^\dagger \hat{s}_n\right)\right\} \\ &+ \frac{1}{4}U_0 a^\dagger a \left[\sqrt{2}\left(\hat{c}_0^\dagger \hat{c}_2 + \hat{c}_2^\dagger \hat{c}_0\right) + \sum_{n\geq 1}^{\infty}\left\{\hat{c}_{n+2}^\dagger \hat{c}_n + \hat{s}_{n+2}^\dagger \hat{s}_n + \hat{c}_n^\dagger \hat{c}_{n+2} + \hat{s}_n^\dagger \hat{s}_{n+2}\right\}\right] \\ &+ \frac{1}{2}\eta_t\left(a^\dagger + a\right)\left[\sqrt{2}\left(\hat{c}_1^\dagger \hat{c}_0 + \hat{c}_0^\dagger \hat{c}_1\right) + \sum_{n\geq 1}^{\infty}\left\{\hat{c}_{n+1}^\dagger \hat{c}_n + \hat{s}_{n+1}^\dagger \hat{s}_n + \hat{c}_n^\dagger \hat{c}_{n+1} + \hat{s}_n^\dagger \hat{s}_{n+1}\right\}\right]. \end{aligned} \tag{1.17}$$

Due to the harmonic potentials in the dispersive interaction terms, we see, that there is no interaction between $\hat{s}_n$ and $\hat{c}_n$ operators and explicitly no interaction between the BEC ground mode $\hat{c}_0^\dagger \hat{c}_0$ and any $\hat{s}_n$ operator. But one can imagine, that we might have a look at those modes, by including any inhomogeneous potential in our Hamiltonian so that we have a scattering process in those modes. However, we can ignore the $\hat{s}_n$ modes in the following steps because we start in the $\hat{c}_0^\dagger \hat{c}_0$ mode and there are no interactions between $\hat{c}_n$ and $\hat{s}_n$ modes.

1.4 Comparison to the two-level Dicke model

In order to compare our expanded model, we can check whether our transformations are correct. Now we should be able to compare the field-operators and of course the Hamiltonian. Beginning with the field operators

$$\hat{\Psi}(x) = \frac{1}{\sqrt{Lp}}\sum_{n=-\infty}^{\infty} b_n e^{ink_0 x} \qquad \text{using (1.9),} \tag{1.18}$$

$$\hat{\Psi}(x) = \frac{1}{\sqrt{Lp}}c_0 + \frac{1}{\sqrt{Lp}}\sum_{n=1}^{\infty}\left[\hat{c}_n cos(nk_0 x) + \hat{s}_n sin(nk_0 x)\right] \tag{1.19}$$

We can reduce the Hilbert space to a two-level system with $n = 0, \pm 1$.

$$\hat{\Psi}(x) = \frac{1}{\sqrt{Lp}}c_0 + \frac{1}{\sqrt{Lp}}\left[\hat{c}_1 cos(k_0 x) + \hat{s}_1 sin(k_0 x)\right] \tag{1.20}$$

Here we can make use of the discussion about the s_n modes in the end of section 1.3 and for $\hat{s}_1 = 0$ the field operator reads like in [7].

Now we can see how the Dicke model emerges from the above (1.17) and the two-level case reduces the model to

$$\begin{aligned} H =& \left(-\Delta_C + \frac{U_0 N}{2}\right)a^\dagger a + \frac{k_0^2}{4m}\left(c_1^\dagger c_1 - c_0^\dagger c_0 + N\right) \\ &+ \frac{1}{4}U_0 N a^\dagger a\left(\frac{1}{2} + \frac{\frac{1}{2}\left(c_1^\dagger c_1 - c_0^\dagger c_0\right)}{N}\right) + \frac{\eta_t}{\sqrt{2}}\left(a^\dagger + a\right)\left(c_1^\dagger c_0 + c_0^\dagger c_1\right) \end{aligned} \tag{1.21}$$

Furthermore we identify the Schwinger representation of SU(2) for the c-modes:

$$c_1^\dagger c_1 + c_0^\dagger c_0 = N; \quad \frac{1}{2}\left(c_1^\dagger c_1 - c_0^\dagger c_0\right) = J_z; \quad \frac{1}{2}\left(c_0^\dagger c_1 + c_1^\dagger c_0\right) = J_x. \tag{1.22}$$

We thus end up with

$$H = \left(-\Delta_C + \frac{U_0 N}{2}\right) a^\dagger a + \frac{k_0^2}{4m}\left(\frac{N}{2} + J_z\right) + \frac{\eta_t}{\sqrt{2}}\left(a^\dagger + a\right) J_x + \frac{1}{4} U_0 N a^\dagger a \left(\frac{1}{2} + \frac{J_z}{2N}\right). \tag{1.23}$$

Renaming the parameters as the energy $\delta_c = \Delta_c - 2u$, the coupling constants $u = \frac{NU_0}{4}$, $y = \sqrt{2N}\eta_t$, the recoil frequency $\omega_R = \frac{k^2}{2m}$ and using a unitary transformation in order to stick to notations

$$a \to \mathrm{i}a \tag{1.24a}$$

$$a^\dagger \to -\mathrm{i}a^\dagger \tag{1.24b}$$

we arive at

$$H = -\delta_c a^\dagger a + \omega_R \left(\underbrace{\frac{N}{2}}_{E} + J_z\right) + \frac{\mathrm{i}y}{\sqrt{N}}\left(a^\dagger - a\right) J_x + u a^\dagger a \left(\frac{1}{2} + \frac{J_z}{N}\right). \tag{1.25}$$

Apart from the underbraced term E, which Nagy et al. in [7] also just neglected, this is the two-level Dicke model.

2 Generalized Holstein-Primakoff transformation

The Holstein-Primakoff mapping is a spin operator representation with bosonic operators. In a two-level system those are expressed by $\hat{S}_- = \sqrt{N - \widetilde{b}_1^\dagger \widetilde{b}_1}\widetilde{b}_1$, $\hat{S}_+ = \widetilde{b}_1^\dagger \sqrt{N - \widetilde{b}_1^\dagger \widetilde{b}_1}$, $\hat{S}_z = \widetilde{b}_1^\dagger \widetilde{b}_1 - \frac{N}{2}$. One can see, that we have to use a more generalized version of that transformation. A more general version is described in [5] and involves two steps: A transformation to $SU(N)$-algebra and based on that the transformation to a generalized Holstein-Primakoff mapping.

2.1 Introducing the transformation to SU(N) algebra

First,we define the transformation to $SU(N)$-mapping.

$$\hat{c}_\nu^\dagger \hat{c}_\mu \equiv A_\nu^\mu \tag{2.1}$$

Now we need to identify the operators in the Hamiltonian (1.17), which leads to

$$
\begin{aligned}
H = -\Delta_C a^\dagger a &+ \frac{1}{2}\sum_{n\geq 1}^{\infty}\left\{\left(n^2k_0^2 + U_0 a^\dagger a\right)\left(A_0^0 + A_n^n\right)\right\} \\
&+ \frac{1}{4}U_0 a^\dagger a\left[\sqrt{2}\left(A_0^2 + A_2^0\right) + A_1^1 + \sum_{n\geq 1}^{\infty}\left\{A_{n+2}^n + A_n^{n+2}\right\}\right] \\
&+ \frac{1}{2}\eta_t\left(a^\dagger + a\right)\left[\sqrt{2}\left(A_1^0 + A_0^1\right) + \sum_{n\geq 1}^{\infty}\left\{A_{n+1}^n + A_n^{n+1}\right\}\right]
\end{aligned}
\tag{2.2}
$$

2.2 Generalized Holstein-Primakoff mapping

We can then define the transformation to the generalized Holstein-Primakoff transformation, where we need to be carefully when defining the ground state of the condensate. In this case it is simply the $\widetilde{b}_0^\dagger\widetilde{b}_0$ mode, hence

$$A_r^s \equiv \widetilde{b}_r^\dagger\widetilde{b}_s, \tag{2.3a}$$

$$A_r^0 \equiv (A_0^r)^\dagger = \widetilde{b}_r^\dagger\Theta(N), \tag{2.3b}$$

$$A_0^0 \equiv (\Theta(N))^2, \tag{2.3c}$$

where

$$\Theta(N) \equiv \sqrt{N - \sum_{m=1}^{n}\widetilde{b}_m^\dagger\widetilde{b}_m}.. \tag{2.3d}$$

$$r, s = 0, 1, 2, ...n. \tag{2.3e}$$

We may then directly refer to Equation (2.2) and identify the Holstein-Primakoff mapping

$$
\begin{aligned}
H = -\Delta_C a^\dagger a + \frac{1}{2}U_0 a^\dagger a\left(\Theta\left(N\right)\right)^2 &+ \sum_{n\geq 1}^{\infty}\left\{\widetilde{b}_n^\dagger\widetilde{b}_n\left(\frac{1}{2}U_0 a^\dagger a + \frac{\hbar k_0^2}{2m}n^2\right)\right\} \\
+ \frac{1}{4}U_0 a^\dagger a&\left[\sqrt{2}\left(\Theta(N)\widetilde{b}_2 + \widetilde{b}_2^\dagger\Theta(N)\right) + \widetilde{b}_1^\dagger\widetilde{b}_1 + \sum_{n\geq 1}^{\infty}\left\{\widetilde{b}_{n+2}^\dagger\widetilde{b}_n + \widetilde{b}_n^\dagger\widetilde{b}_{n+2}\right\}\right] \\
+ \frac{1}{2}\eta(a^\dagger + a)&\left[\sqrt{2}\left(\Theta(N)\widetilde{b}_1 + \widetilde{b}_1^\dagger\Theta(N)\right) + \sum_{n\geq 1}^{\infty}\left\{\widetilde{b}_{n+1}^\dagger\widetilde{b}_n + \widetilde{b}_n^\dagger\widetilde{b}_{n+1}\right\}\right].
\end{aligned}
\tag{2.4}
$$

Evaluating the $(\Theta(N))^2$ leads to the final result of this chapter

$$
\begin{aligned}
H = & -\Delta_C a^\dagger a + \frac{1}{2} U_0 a^\dagger a \left\{ N + \frac{1}{2} \widetilde{b}_1^\dagger \widetilde{b}_1 \right\} + \sum_{n\geq 1}^{\infty} \frac{\hbar k_0^2}{2m} n^2 \widetilde{b}_n^\dagger \widetilde{b}_n \\
& + \frac{1}{4} U_0 a^\dagger a \left[\sqrt{2} \left\{ \Theta(N) \widetilde{b}_2 + \widetilde{b}_2^\dagger \Theta(N) \right\} + \sum_{n\geq 1}^{\infty} \left\{ \widetilde{b}_{n+2}^\dagger \widetilde{b}_n + \widetilde{b}_n^\dagger \widetilde{b}_{n+2} \right\} \right] \\
& + \frac{1}{2} \eta (a^\dagger + a) \left[\sqrt{2} \left\{ \Theta(N) \widetilde{b}_1 + \widetilde{b}_1^\dagger \Theta(N) \right\} + \sum_{n\geq 1}^{\infty} \left\{ \widetilde{b}_{n+1}^\dagger \widetilde{b}_n + \widetilde{b}_n^\dagger \widetilde{b}_{n+1} \right\} \right]
\end{aligned}
\tag{2.5}
$$

What we can see again is, that due to the special treatment of the condensate ground-state and the interaction between the level $\hat{c}_0$ and $\hat{c}_2$ we get two of the interesting Θ terms. Those terms including Θ describe mainly an interaction between the condensate ground-state and any excited state. Those interactions are interesting because they must be the most used ones at the phase transition. However, at this point it is confirmed, that our expectation - the interaction between n and $n+2$ - plays a major role in the phase transition.

2.3 Comparison to the Holstein-Primakoff mapped, two-level Dicke-model

As before, we can check the Hamiltonian (2.5) with the two-level Dicke Hamiltonian in Holstein-Primakoff mapping. To compare this Hamiltonian we reduce the modes to $n = \{0, 1\}$ and ignore all other Levels.

$$
H = -\Delta_C a^\dagger a + \frac{1}{2} U_0 a^\dagger a \left\{ N + \frac{1}{2} \widetilde{b}_1^\dagger \widetilde{b}_1 \right\} + \frac{\hbar k_0^2}{2m} \widetilde{b}_1^\dagger \widetilde{b}_1 + \frac{1}{2} \eta (a^\dagger + a) \left[\sqrt{2} \left\{ \Theta(N) \widetilde{b}_1 + \widetilde{b}_1^\dagger \Theta(N) \right\} \right], \tag{2.6}
$$

where we can do the replacements again: the energy $\delta_c = \Delta_c - 2u$, the coupling constants $u = \frac{NU_0}{4}$, $y = \sqrt{2N}\eta_t$, and the recoil frequency $\omega_R = \frac{k^2}{2m}$. Considering the unitary transformation (1.24a) leads to

$$
H = -\delta_c a^\dagger a + \omega_R \widetilde{b}_1^\dagger \widetilde{b}_1 + \frac{u}{N} a^\dagger a \widetilde{b}_1^\dagger \widetilde{b}_1 + \frac{\mathrm{i}}{2} y \left(a^\dagger - a \right) \left\{ \widetilde{b}_1^\dagger \sqrt{1 - \frac{\widetilde{b}_1^\dagger \widetilde{b}_1}{N}} + \sqrt{1 - \frac{\widetilde{b}_1^\dagger \widetilde{b}_1}{N}} \widetilde{b}_1 \right\}. \tag{2.7}
$$

The Equation (2.7) is the two-level Dicke Hamiltonian in Holstein-Primakoff mapping recently derived in reference [7].

3 Displaced harmonic oscillator

3.1 Displacement operators

As shown in [4] we can now derive an effective model considering the super-radiant system as a displaced harmonic oscillator. The normal-phase is then more a by-product of the following calculations. A faster way to receive the effective model in the normal-phase is described in [4].

Let us start with the Holstein-Primakoff mapped Hamiltonian (2.5) and replace the factors

$$\delta_C = \Delta_C - 2u, \quad u = \frac{NU_0}{4}, \quad y = \sqrt{2N}\eta_t, \quad \omega_R = k_0^2, \tag{3.1}$$

as shown before. Using the displacement operators

$$a^\dagger \longmapsto e^\dagger + \sqrt{\alpha} \tag{3.2a}$$

$$\tilde{b}_n^\dagger \longmapsto d_n^\dagger + \sqrt{\beta} \tag{3.2b}$$

the Hamiltonian transforms to

$$\begin{aligned}
H = &-\delta_C \left(e^\dagger e + \sqrt{\alpha}\left(e^\dagger + e\right) + \alpha\right) + \frac{u}{N}\left(e^\dagger e + \sqrt{\alpha}\left(e^\dagger + e\right) + \alpha\right)\left[d_1^\dagger d_1 + \sqrt{\beta_1}\left(d_1^\dagger + d_1\right) + \beta_1\right] \\
&+ \sum_{n\geq 1}^{\infty} \omega_r n^2 \left(d_n^\dagger d_n + \sqrt{\beta_n}\left(d_n^\dagger + d_n\right) + \beta_n\right) + \frac{y\sqrt{k}}{2\sqrt{N}}\left(e^\dagger + e + 2\sqrt{\alpha}\right)\left[d_1^\dagger \tilde{\Theta} + \tilde{\Theta} d_1 + 2\sqrt{\beta_1}\tilde{\Theta}\right] \\
&+ \frac{y}{2\sqrt{2N}}\left(e^\dagger + e + 2\sqrt{\alpha}\right) \\
&\left[\sum_{n\geq 1}^{\infty} d_{n+1}^\dagger d_n + d_n^\dagger d_{n+1} + \sqrt{\beta_{n+1}}\left(d_n^\dagger + d_n\right) + \sqrt{\beta_n}\left(d_{n+1}^\dagger + d_{n+1}\right) + 2\sqrt{\beta_{n+1}\beta_n}\right] \\
&+ \frac{u}{N}\sqrt{2k}\left(e^\dagger e + \sqrt{\alpha}\left(e^\dagger + e\right) + \alpha\right)\left[d_2^\dagger \tilde{\Theta} + \tilde{\Theta} d_2 + 2\sqrt{\beta_2}\tilde{\Theta}\right] + \frac{u}{N}\left(e^\dagger e + \sqrt{\alpha}\left(e^\dagger + e\right) + \alpha\right) \\
&\left[\sum_{n\geq 1}^{\infty} d_{n+2}^\dagger d_n + d_n^\dagger d_{n+2} + \sqrt{\beta_{n+2}}\left(d_n^\dagger + d_n\right) + \sqrt{\beta_n}\left(d_{n+2}^\dagger + d_{n+2}\right) + 2\sqrt{\beta_{n+2}\beta_n}\right]
\end{aligned} \tag{3.3}$$

where $\tilde{\Theta}$ is extracted from the term (2.3d), as shown below

$$\Theta = \sqrt{N - \sum_{n\geq 1}^{\infty}\left(d_n^\dagger + \sqrt{\beta_n}\right)\left(d_n + \sqrt{\beta_n}\right)} \tag{3.4}$$

$$= \sqrt{\underbrace{N - \sum_{n\geq 1}^{\infty}\beta_n}_{k} - \sum_{n\geq 1}^{\infty} d_n^\dagger d_n + \sqrt{\beta_n}\left(d_n^\dagger + d_n\right)} \tag{3.5}$$

$$= \sqrt{k}\underbrace{\sqrt{1 - \sum_{n\geq 1}^{\infty}\frac{d_n^\dagger d_n + \sqrt{\beta_n}\left(d_n^\dagger + d_n\right)}{k}}}_{\tilde{\Theta}} = \sqrt{k}\tilde{\Theta} \tag{3.6}$$

$$\tilde{\Theta} = \sqrt{1 - \sum_{n\geq 1}^{\infty}\frac{d_n^\dagger d_n + \sqrt{\beta_n}\left(d_n^\dagger + d_n\right)}{k}}. \tag{3.7}$$

We explicitly define $k = N - \sum_{n\geq 1}^{\infty}\beta_n$ and for simplicity let us introduce $x_n = d_n^\dagger d_n + \sqrt{\beta_n}\left(d_n^\dagger + d_n\right)$.

3.2 Thermodynamic limit

In the thermodynamic limit we may expand the root to the second order

$$\tilde{\Theta} = \sqrt{1 - \sum_{n\geq 1}^{\infty} \frac{x_n}{k}} = 1 - \frac{1}{2}\sum_{n\geq 1}^{\infty} \frac{x_n}{k} - \frac{1}{8}\left(\sum_{n\geq 1}^{\infty} \frac{x_n}{k}\right)^2 + \mathcal{O}^3\left(\frac{x_n}{k}\right) \tag{3.8}$$

We are neglecting the terms of $\mathcal{O}\left(\left(\frac{x_n}{k}\right)^3\right)$ and higher, so that evaluating the term $\frac{1}{8}\left(\sum_{n\geq 1}^{\infty} \frac{x_n}{k}\right)^2$ gives

$$\frac{1}{8}\left(\sum_{n\geq 1}^{\infty} \frac{x_n}{k}\right)^2 = \frac{1}{8k^2}\left(\sum_{n\geq 1}^{\infty} d_n^\dagger d_n + \sqrt{\beta_n}\left(d_n^\dagger + d_n\right)\right)\left(\sum_{n'\geq 1}^{\infty} d_{n'}^\dagger d_{n'} + \sqrt{\beta_{n'}}\left(d_{n'}^\dagger + d_{n'}\right)\right) \tag{3.9}$$

$$\begin{aligned} &= \frac{1}{8k^2}\sum_{n,n'\geq 1}^{\infty}\Big\{d_n^\dagger d_n d_{n'}^\dagger d_{n'} + d_n^\dagger d_n \sqrt{\beta_{n'}}\left(d_{n'}^\dagger + d_{n'}\right) + \sqrt{\beta_n}\left(d_n^\dagger + d_n\right) d_{n'}^\dagger d_{n'} \\ &+ \sqrt{\beta_n \beta_{n'}}\left(d_n^\dagger d_{n'}^\dagger + d_n d_{n'} + d_n^\dagger d_{n'} + d_n d_{n'}^\dagger\right)\Big\}. \end{aligned} \tag{3.10}$$

For the thermodynamic limit of the Hamiltonian, we need to consider the proportionalities, that are pointed out next:

$$k \propto N \qquad \beta_n \propto N \qquad \alpha \propto N \tag{3.11}$$

$$d_n^\dagger d_n \propto 1 \qquad u \propto 1 \qquad \delta_C \propto 1 \tag{3.12}$$

$$\omega_R \propto 1 \qquad n^2 \propto 1 \qquad y \propto 1 \tag{3.13}$$

We can then identify the term specific scaling with N, which is emphasized with the curly brackets.

$$
\begin{aligned}
H = &-\underbrace{\delta_C}_{1}\left(\underbrace{e^{\dagger}e}_{1}+\underbrace{\sqrt{\alpha}\left(e^{\dagger}+e\right)}_{\sqrt{N}}+\underbrace{\alpha}_{N}\right)+\sum_{n\geq 1}^{\infty}\underbrace{\omega_r n^2}_{1}\left(\underbrace{d_n^{\dagger}d_n}_{1}+\underbrace{\sqrt{\beta_n}\left(d_n^{\dagger}+d_n\right)}_{\sqrt{N}}+\underbrace{\beta_n}_{N}\right)\\
&+\underbrace{\frac{u}{N}}_{\frac{1}{N}}\left(\underbrace{e^{\dagger}e}_{1}+\underbrace{\sqrt{\alpha}\left(e^{\dagger}+e\right)}_{\sqrt{N}}+\underbrace{\alpha}_{N}\right)\left[\underbrace{d_1^{\dagger}d_1}_{1}+\underbrace{\sqrt{\beta_1}\left(d_1^{\dagger}+d_1\right)}_{\sqrt{N}}+\underbrace{\beta_1}_{N}\right]\\
&+\underbrace{\frac{y\sqrt{k}}{2\sqrt{N}}}_{1}\left(\underbrace{e^{\dagger}+e}_{1}+2\underbrace{\sqrt{\alpha}}_{\sqrt{N}}\right)\left[d_1^{\dagger}\tilde{\Theta}+\tilde{\Theta}d_1+2\underbrace{\sqrt{\beta_1}}_{\sqrt{N}}\tilde{\Theta}\right]+\underbrace{\frac{y}{2\sqrt{2N}}}_{\frac{1}{\sqrt{N}}}\left(\underbrace{e^{\dagger}+e}_{1}+\underbrace{2\sqrt{\alpha}}_{\sqrt{N}}\right)\\
&\left[\sum_{n\geq 1}^{\infty}\underbrace{d_{n+1}^{\dagger}d_n+d_n^{\dagger}d_{n+1}}_{1}+\underbrace{\sqrt{\beta_{n+1}}\left(d_n^{\dagger}+d_n\right)+\sqrt{\beta_n}\left(d_{n+1}^{\dagger}+d_{n+1}\right)}_{\sqrt{N}}+\underbrace{2\sqrt{\beta_{n+1}\beta_n}}_{N}\right]\\
&+\underbrace{\frac{u\sqrt{2k}}{N}}_{\frac{1}{\sqrt{N}}}\left(\underbrace{e^{\dagger}e}_{1}+\underbrace{\sqrt{\alpha}\left(e^{\dagger}+e\right)}_{\sqrt{N}}+\underbrace{\alpha}_{N}\right)\left[d_2^{\dagger}\tilde{\Theta}+\tilde{\Theta}d_2+2\underbrace{\sqrt{\beta_2}}_{\sqrt{N}}\tilde{\Theta}\right]\\
&+\underbrace{\frac{u}{N}}_{\frac{1}{N}}\left(\underbrace{e^{\dagger}e}_{1}+\underbrace{\sqrt{\alpha}\left(e^{\dagger}+e\right)}_{\sqrt{N}}+\underbrace{\alpha}_{N}\right)\\
&\left[\sum_{n\geq 1}^{\infty}\underbrace{d_{n+2}^{\dagger}d_n+d_n^{\dagger}d_{n+2}}_{1}+\underbrace{\sqrt{\beta_{n+2}}\left(d_n^{\dagger}+d_n\right)+\sqrt{\beta_n}\left(d_{n+2}^{\dagger}+d_{n+2}\right)}_{\sqrt{N}}+\underbrace{2\sqrt{\beta_{n+2}\beta_n}}_{N}\right]
\end{aligned}
\tag{3.14}
$$

In the interest of clarity I handle the $\tilde{\Theta}$ terms separately.

$$
\begin{aligned}
\tilde{\Theta} = 1 &- \underbrace{\frac{1}{2k}}_{\frac{1}{N}}\sum_{n\geq 1}^{\infty}\left[\underbrace{d_n^{\dagger}d_n}_{1}+\underbrace{\sqrt{\beta_n}\left(d_n^{\dagger}+d_n\right)}_{\sqrt{N}}\right]-\underbrace{\frac{1}{8k^2}}_{\frac{1}{N^2}}\sum_{n,n'\geq 1}^{\infty}\left[\underbrace{d_n^{\dagger}d_n d_{n'}^{\dagger}d_{n'}}_{1}+\underbrace{d_n^{\dagger}d_n\sqrt{\beta_{n'}}\left(d_{n'}^{\dagger}+d_{n'}\right)}_{\sqrt{N}}\right.\\
&\left.+\underbrace{\sqrt{\beta_n}\left(d_n^{\dagger}+d_n\right)d_{n'}^{\dagger}d_{n'}}_{\sqrt{N}}+\underbrace{\sqrt{\beta_n\beta_{n'}}\left(d_n^{\dagger}+d_n\right)\left(d_{n'}^{\dagger}+d_{n'}\right)}_{N}\right]
\end{aligned}
\tag{3.15}
$$

Now we neglect terms with overall powers of N in the denominator, so that we obtain

$$
\begin{aligned}
H =& -\delta_C \left(e^\dagger e + \sqrt{\alpha}\left(e^\dagger + e\right) + \alpha\right) + \sum_{n\geq 1}^{\infty} \omega_r n^2 \left[d_n^\dagger d_n + \sqrt{\beta_n}\left(d_n^\dagger + d_n\right) + \beta_n\right] \\
&+ \frac{u}{N} e^\dagger e \beta_1 + \frac{u}{N}\left(\sqrt{\alpha}\left(e^\dagger + e\right)\right)\left[\sqrt{\beta_1}\left(d_1^\dagger + d_1\right) + \beta_1\right] + \frac{u\alpha}{N}\left[d_1^\dagger d_1 + \sqrt{\beta_1}\left(d_1^\dagger + d_1\right) + \beta_1\right] \\
&+ \frac{y\sqrt{k}}{2\sqrt{N}}\left(e^\dagger + e\right)\left[d_1^\dagger + d_1 + 2\sqrt{\beta_1}\left(1 - \frac{1}{2k}\sum_{n\geq 1}^{\infty}\sqrt{\beta_n}\left(d_n^\dagger + d_n\right)\right)\right] \\
&+ \frac{y\sqrt{k\alpha}}{\sqrt{N}}\left[d_1^\dagger\left(1 - \frac{1}{2k}\sum_{n\geq 1}^{\infty}\sqrt{\beta_n}\left(d_n^\dagger + d_n\right)\right) + \left(1 - \frac{1}{2k}\sum_{n\geq 1}^{\infty}\sqrt{\beta_n}\left(d_n^\dagger + d_n\right)\right) d_1\right. \\
&\left. + 2\sqrt{\beta_1}\left(1 - \frac{1}{2k}\sum_{n\geq 1}^{\infty}\left\{d_n^\dagger d_n + \sqrt{\beta_n}\left(d_n^\dagger + d_n\right)\right\}\right)\right] \\
&- \sum_{n,n'\geq 1}^{\infty}\frac{y\sqrt{\alpha\beta_1\beta_n\beta_{n'}}}{4\sqrt{Nk^3}}\left(d_n^\dagger + d_n\right)\left(d_{n'}^\dagger + d_{n'}\right) - \sum_{n,n'\geq 1}^{\infty}\frac{u\alpha\sqrt{2\beta_2\beta_n\beta_{n'}}}{4N\sqrt{k^3}}\left(d_n^\dagger + d_n\right)\left(d_{n'}^\dagger + d_{n'}\right) \\
&+ \sum_{n\geq 1}^{\infty}\frac{y}{2\sqrt{2N}}\left(e^\dagger + e\right)\left[\sqrt{\beta_{n+1}}\left(d_n^\dagger + d_n\right) + \sqrt{\beta_n}\left(d_{n+1} + d_{n+1}\right) + 2\sqrt{\beta_{n+1}\beta_n}\right] \\
&+ \sum_{n\geq 1}^{\infty}\frac{y\sqrt{\alpha}}{\sqrt{2N}}\left[d_{n+1}^\dagger d_n + d_n^\dagger d_{n+1} + \sqrt{\beta_{n+1}}\left(d_n^\dagger + d_n\right) + \sqrt{\beta_n}\left(d_{n+1}^\dagger + d_{n+1}\right) + 2\sqrt{\beta_{n+1}\beta_n}\right] \\
&+ \frac{u\sqrt{2k\alpha}}{N}\left(e^\dagger + e\right)\left[d_2^\dagger + d_2 + 2\sqrt{\beta_2}\left(1 - \frac{1}{2k}\sum_{n\geq 1}^{\infty}\sqrt{\beta_n}\left(d_n^\dagger + d_n\right)\right)\right] + \frac{2u\sqrt{2k\beta_2}}{N} e^\dagger e \\
&+ \frac{u\alpha\sqrt{2k}}{N}\left[d_2^\dagger\left(1 - \frac{1}{2k}\sum_{n\geq 1}^{\infty}\sqrt{\beta_n}\left(d_n^\dagger + d_n\right)\right) + \left(1 - \frac{1}{2k}\sum_{n\geq 1}^{\infty}\sqrt{\beta_n}\left(d_n^\dagger + d_n\right)\right) d_2\right. \\
&\left. + 2\sqrt{\beta_2}\left(1 - \frac{1}{2k}\sum_{n\geq 1}^{\infty}\left\{d_n^\dagger d_n + \sqrt{\beta_n}\left(d_n^\dagger + d_n\right)\right\}\right)\right] + \sum_{n\geq 1}^{\infty}\frac{2u}{N} e^\dagger e\sqrt{\beta_{n+2}\beta_n} \\
&+ \sum_{n\geq 1}^{\infty}\frac{u\sqrt{\alpha}}{N}\left(e^\dagger + e\right)\left[\sqrt{\beta_{n+2}}\left(d_n^\dagger + d_n\right) + \sqrt{\beta_n}\left(d_{n+2}^\dagger + d_{n+2}\right) + 2\sqrt{\beta_{n+2}\beta_n}\right] \\
&+ \sum_{n\geq 1}^{\infty}\frac{u\alpha}{N}\left[d_{n+2}^\dagger d_n + d_n^\dagger d_{n+2} + \sqrt{\beta_{n+2}}\left(d_n^\dagger + d_n\right) + \sqrt{\beta_n}\left(d_{n+2}^\dagger + d_{n+2}\right) + 2\sqrt{\beta_{n+2}\beta_n}\right].
\end{aligned}
\tag{3.16}
$$

This complex interacting Hamiltonian may now be simplified by eliminating all terms in $\mathcal{O}\left(\sqrt{N}\right)$, those are linear in the bosonic operators. We may also conclude, that terms, which are in $\mathcal{O}(1)$ contribute to the mode energy or interaction energy and terms in $\mathcal{O}(N)$ bring a constant energy offset.

4 Effective Hamiltonians

4.1 Finding solutions

To derive the effective Hamiltonians we need to solve the displacement factors α, β_n, such that the terms in (3.16), which are linear in the bosonic operators vanish. This is analogous to a displaced harmonic oscillator. An easy way to get these equations is to consider, that they are scaling with $\mathcal{O}\left(\sqrt{N}\right)$.

$$
\begin{aligned}
H^{\frac{1}{2}} = & \left(e^\dagger + e\right) \\
& \left\{ \underbrace{-\delta_C\sqrt{\alpha} + \frac{u\sqrt{\alpha}}{N}\left[\beta_1 + 2\sqrt{2k\beta_2} + 2\sum_{n\geq 1}^{\infty}\sqrt{\beta_{n+2}\beta_n}\right] + \frac{y}{\sqrt{N}}\left[\sqrt{k\beta_1} + \sum_{n\geq 1}^{\infty}\sqrt{\frac{\beta_{n+1}\beta_n}{2}}\right]}_{=0} \right\} \\
& + \left(d_1^\dagger + d_1\right)\left\{ \underbrace{\omega_r\sqrt{\beta_1} + \frac{u\alpha}{N}\left[\sqrt{\beta_1} - \sqrt{\frac{2\beta_2\beta_1}{k}} + \sqrt{\beta_3}\right] + \frac{y\sqrt{\alpha}}{\sqrt{N}}\left[\sqrt{\frac{\beta_2}{2}} + \sqrt{k} - \frac{\beta_1}{\sqrt{k}}\right]}_{=0} \right\} \\
& + \left(d_2^\dagger + d_2\right)\left\{ \underbrace{4\omega_r\sqrt{\beta_2} + \frac{u\alpha}{N}\left[\sqrt{2k} - \frac{\sqrt{2}\beta_2}{\sqrt{k}} + \sqrt{\beta_4}\right] + \frac{y\sqrt{\alpha}}{\sqrt{N}}\left[\sqrt{\frac{\beta_1}{2}} + \sqrt{\frac{\beta_3}{2}} - \sqrt{\frac{\beta_1\beta_2}{k}}\right]}_{=0} \right\} \\
& + \sum_{n\geq 3}^{\infty}\left(d_n^\dagger + d_n\right) \\
& \left\{ \underbrace{\omega_r n^2\sqrt{\beta_n} - \frac{y\sqrt{\alpha}}{\sqrt{N}}\left[\sqrt{\frac{\beta_1\beta_n}{k}} - \sqrt{\frac{\beta_{n+1}}{2}} - \sqrt{\frac{\beta_{n-1}}{2}}\right] + \frac{u\alpha}{N}\left[\sqrt{\beta_{n+2}} + \sqrt{\beta_{n-2}} - \sqrt{\frac{2\beta_2\beta_n}{k}}\right]}_{=0} \right\}
\end{aligned}
\tag{4.1}
$$

The trivial solution leads to the normal phase Hamiltonian, that is analytically treated in the following section 4.2.

The super-radiant phase is caused by non-trivial, real solutions of this non-linear system of equations. The system can be solved numerically and because of this we will consider different cases by cutting of at the level n_{cutoff}. So the super-radiant phase is treated in the section 4.3.

4.2 Normal phase

As shown in [4], we obtain the normal phase Hamiltonian by setting α, β_n to zero. The trivial solution reduces the Hamiltonian then to.

$$H = -\delta_C a^\dagger a + \sum_{n\geq 1}^{\infty}\omega_r n^2 \widetilde{b}_n^\dagger \widetilde{b}_n + \frac{y}{2}\left(a^\dagger + a\right)\left[\widetilde{b}_1^\dagger + \widetilde{b}_1\right] \tag{4.2}$$

As one can see, the bosonic creation and annihilation operators have changed back to the generalized Holstein-Primakoff mapping introduced in (2.3a). The physical interesting fact is, that the cavity field only couples the first excited state of the BEC. So the two-level Dicke model is exact in the normal phase. In order to receive excitation energies in the normal phase, we may introduce $y_{crit} = \sqrt{-\delta_C \omega_R}$ and construct the Hamiltonian (4.2) in terms of quadratic forms as

$$M = \begin{pmatrix} \delta_C^2 & y \cdot y_{crit} & 0 & \dots & 0 \\ y \cdot y_{crit} & \omega_R^2 & 0 & \dots & 0 \\ 0 & 0 & 16\omega_R^2 & \dots & 0 \\ 0 & \dots & 0 & \ddots & 0 \\ 0 & \dots & \dots & 0 & n^4\omega_R^2 \end{pmatrix}. \tag{4.3}$$

It is then possible to diagonalize the first block, which leads to

$$\omega_\pm^2 = \frac{\delta_C^2 + \omega_R^2}{2} \pm \sqrt{\left(\frac{\delta_C^2 - \omega_R^2}{2}\right)^2 + 4y^2 y_{crit}^2} \tag{4.4}$$

ω_- goes to zero at $y = y_{crit}$, which shows that the energy of the photonic mode vanishes. This

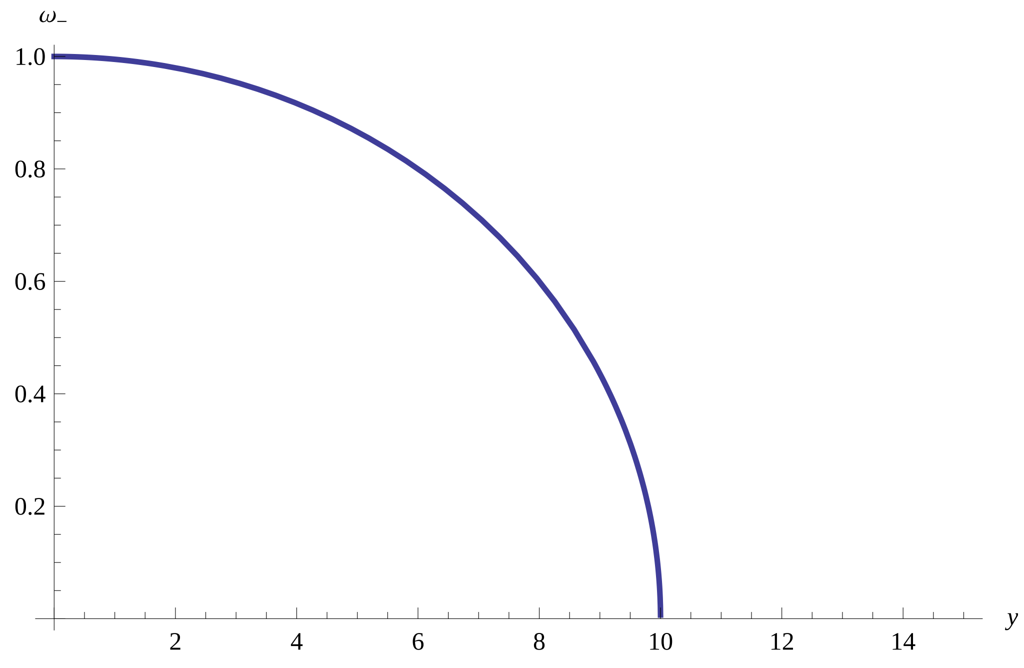

Figure 3: Illustration of the ω_- frequenzy branch. It shows, that the frequency ω_- goes to zero at the critical pump strength $y_{crit} = 10$, while is $\delta_C = 100$ and $\omega_r = 1$

shows the similarity to the normal Dicke model and indicates, that the phase transition occurs in multi-level Dicke model.

4.3 Super-radiant phase

4.3.1 $n_{cutoff} = 1$ - The two-level Dicke model.

The equations from (4.1) may be written in the following way for a two-level model.

$$\delta_C \sqrt{\alpha} + \frac{u\sqrt{\alpha}\beta_1}{N} + \frac{y\sqrt{k\beta_1}}{\sqrt{N}} = 0 \tag{4.5a}$$

$$\omega_r \sqrt{\beta_1} + \frac{u\alpha\sqrt{\beta_1}}{N} + \frac{y\sqrt{\alpha}}{\sqrt{N}}\left[\sqrt{k} - \frac{\beta_1}{\sqrt{k}}\right] = 0 \tag{4.5b}$$

We may then use the transformation

$$\sqrt{\alpha} = \sqrt{N}\tilde{\alpha}, \tag{4.6a}$$

$$\sqrt{\beta_1} = \sqrt{N}\tilde{\beta}_1 \tag{4.6b}$$

in order to correctly scale with the fixed number of particles N.
k reduces to

$$k = N - \beta_1 \tag{4.7a}$$

$$N\tilde{k} = 1 - \tilde{\beta_1}^2. \tag{4.7b}$$

The equations (4.5a) can then be written as

$$\left(\delta_C + u\beta_1^2\right)\tilde{\alpha} = -y\tilde{\beta}_1\sqrt{1-\tilde{\beta}_1^2}, \tag{4.8}$$

$$\left(\omega_R + u\tilde{\alpha}^2\right)\tilde{\beta}_1 = -y\tilde{\alpha}\left(\frac{1-2\tilde{\beta}_1^2}{\sqrt{1-\tilde{\beta}_1^2}}\right), \tag{4.9}$$

which can be compared to the article [7]. The solutions of the equation system (4.8) are not all physically interesting. However, we may interpret $\tilde{\beta}_n^2$ as the result of $< d_n^\dagger d_n >$ as shown in [6], hence we may reduce the solutions to $0 < \tilde{\beta}_n^2 \leq 1$.
It is then possible to illustrate the super-radiant phase above the point y_{crit} and see how the cavity mode a evolves in the super-radiant phase (Figure 4).

4.3.2 $n_{cutoff} = 5$ - The multi-level Dicke model.

Again, let us start with (4.1) which may be reduced to a five-level system. In order to see the scaling in α and β_n more easily, we may prefer to write

$$\sqrt{\alpha} \to \sqrt{N}\tilde{\alpha} \tag{4.10a}$$

$$\sqrt{\beta_n} \to \sqrt{N}\tilde{\beta}_n \tag{4.10b}$$

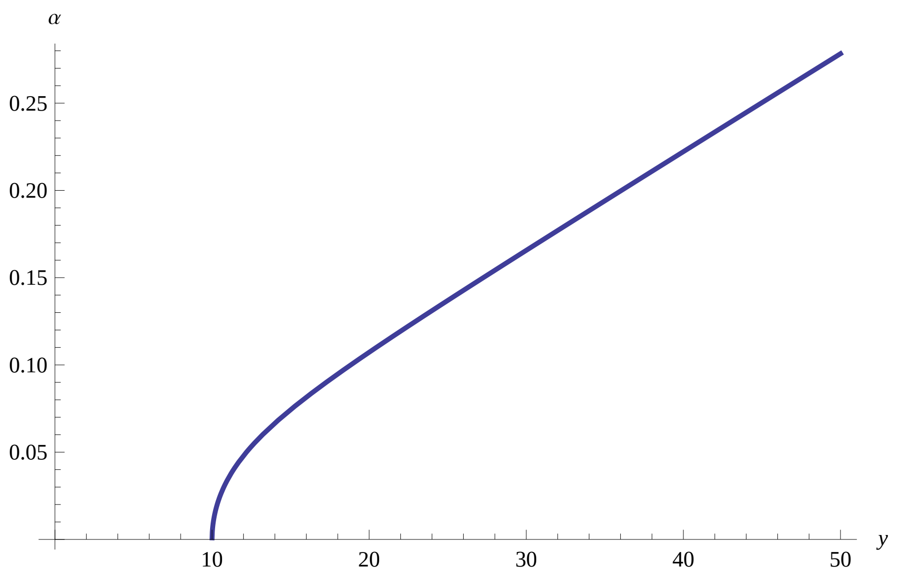

Figure 4: We can see the solution of α as a function of y, which is the laser pumping strength. The plotted solution is only viable in the super-radiant phase and illustrates the phase-transition at $y_{crit} = 10$. Comparable to [7]

In this notation we may write k as

$$k = N - \sum_{n\geq}^{n_{cutoff}} \beta_n \tag{4.11a}$$

$$N\tilde{k} = 1 - \sum_{n\geq 1}^{n_{cutoff}} \tilde{\beta}_n{}^2 \tag{4.11b}$$

and the equations multiplied with $\sqrt{N\tilde{k}}$ read

$$-\delta_C\tilde{\alpha} + u\tilde{\alpha}\left[\tilde{\beta}_1^2 + 2\sqrt{2\tilde{k}}\tilde{\beta}_2 + \tilde{\beta}_3\tilde{\beta}_1 + \tilde{\beta}_4\tilde{\beta}_2\right] + y\left[\sqrt{\tilde{k}}\tilde{\beta}_1 + \sqrt{\frac{1}{2}}\left(\tilde{\beta}_2\tilde{\beta}_1 + \tilde{\beta}_2\tilde{\beta}_3 + \tilde{\beta}_3\tilde{\beta}_4\right)\right] = 0 \tag{4.12a}$$

$$\sqrt{\tilde{k}}\omega_r\tilde{\beta}_1 + u\tilde{\alpha}^2\left[\sqrt{\tilde{k}}\tilde{\beta}_1 - \sqrt{2}\tilde{\beta}_2\tilde{\beta}_1 + \sqrt{\tilde{k}}\tilde{\beta}_3\right] + y\tilde{\alpha}\left[\sqrt{\frac{\tilde{k}}{2}}\tilde{\beta}_2 + \tilde{k} - \tilde{\beta}_1^2\right] = 0 \tag{4.12b}$$

$$4\sqrt{\tilde{k}}\omega_r\tilde{\beta}_2 + u\tilde{\alpha}^2\left[\sqrt{2\tilde{k}} - \sqrt{2}\tilde{\beta}_2^2 + \sqrt{\tilde{k}}\tilde{\beta}_4\right] + y\tilde{\alpha}\left[\sqrt{\frac{\tilde{k}}{2}}\left(\tilde{\beta}_1 + \tilde{\beta}_3\right) - \tilde{\beta}_1\tilde{\beta}_2\right] = 0 \tag{4.12c}$$

$$9\sqrt{\tilde{k}}\omega_R\tilde{\beta}_3 - y\tilde{\alpha}\left[\tilde{\beta}_1\tilde{\beta}_3 - \sqrt{\frac{k}{2}}\left(\tilde{\beta}_2 + \tilde{\beta}_4\right)\right] + u\tilde{\alpha}^2\left[\sqrt{\tilde{k}}\tilde{\beta}_1 - \sqrt{2}\tilde{\beta}_2\tilde{\beta}_3\right] = 0 \tag{4.12d}$$

$$16\sqrt{\tilde{k}}\omega_R\tilde{\beta}_4 - y\tilde{\alpha}\left[\tilde{\beta}_1\tilde{\beta}_4 - \sqrt{\frac{k}{2}}\tilde{\beta}_3\right] + u\tilde{\alpha}^2\left[\sqrt{\tilde{k}}\tilde{\beta}_2 - \sqrt{2}\tilde{\beta}_2\tilde{\beta}_4\right] = 0 \tag{4.12e}$$

Though we can not solve this system analytically we need to solve those non-linear equations numerically. Therefore, we start finding solutions in the super-radiant phase and follow those solutions by iterating the factor y. Once a solution is found, we may follow it and illustrate the super-radiant phase, the phase transition and the normal-phase. We see, that the phase-transition

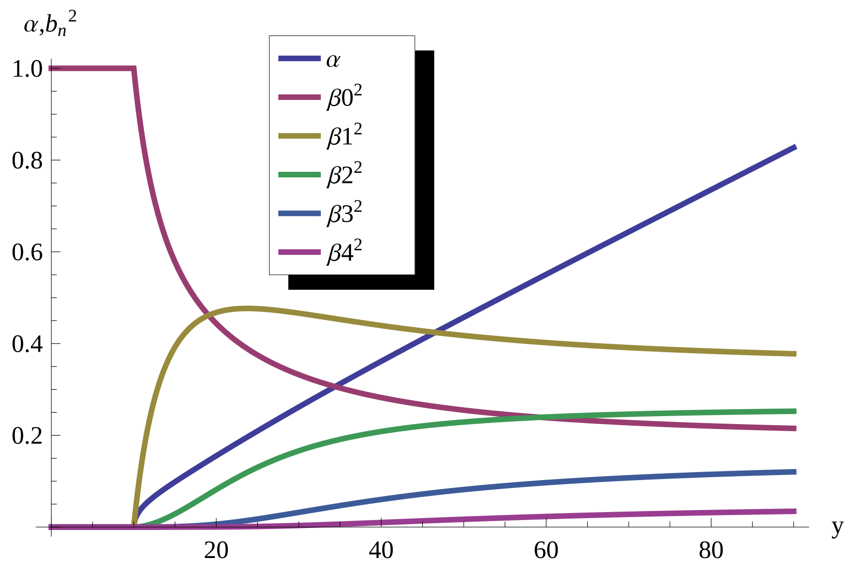

Figure 5: Illustration of the mode population as a function of the pumping strenght y. With slight differences comparable to [6].

occurs mainly in the $d_0^\dagger d_0$ and $d_1^\dagger d_1$ modes. Above the threshold $y_{crit} = 10$ other modes get involved and for high y the solutions of this system converge to constant parameters.
If we compare the results with the recently found ones in [6], we find out, that there are slight differences in the behavior of the mode population. The differences can be explained by two things. We are using a different numerical way to create the solutions for α and β_n and the mean-field method may produce slight different results.

5 Conclusions and outlook

This thesis shows a generalized Holstein-Primakoff transformation leading to a multi-level Dicke model. The complex mode structure brings a non-linear system of equations, which needs to be solved numerically. However, the population of the cavity mode and several other BEC modes are shown in the normal-phase as well as in the super-radiant phase. The analysis of the results points out, that it is necessary to consider more modes well above the phase-transition point y_{crit}. The results of the generalized Holstein-Primakoff transformation are exact, when reduced to a two-level system. However, the multi-level system is slightly different to the mean field theory presented in [6].
Sticking to the multi-level Dicke model the next step can be to derive the spectrum. It is also possible to consider other sectors than $q = 0$ and to develop a two dimensional multi-mode model. It would also be interesting to compare the mean field method with the Holstein-Primakoff transformation exactly.
However, it is possible to use this generalized Holstein-Primakoff transformation for other multi-mode expansions.

6 References

[1] Ashcroft, Neil. W and Mermin, N. David. *Solid State Physics.* Cengage Learning Services, 1976.

[2] Kristian Baumann, Christine Guerlin, Ferdinand Brennecke, and Tilman Esslinger. Dicke quantum phase transition with a superfluid gas in an optical cavity. *Nature*, 464(7293):1301–1306, Apr 2010.

[3] R. H. Dicke. Coherence in spontaneous radiation processes. *Phys. Rev.*, 93(1):99, Jan 1954.

[4] Clive Emary and Tobias Brandes. Chaos and the quantum phase transition in the dicke model. *Phys. Rev. E*, 67(6):066203, Jun 2003.

[5] Abraham Klein and E. R. Marshalek. Boson realizations of lie algebras with applications to nuclear physics. *Rev. Mod. Phys.*, 63(2):375–558, Apr 1991.

[6] G. Kónya, G. Szirmai, and P. Domokos. Multimode mean-field model for the quantum phase transition of a bose-einstein condensate in an optical resonator. *arXiv.org*, 1101(3760v1), Jan 2011.

[7] D. Nagy, G. Kónya, G. Szirmai, and P. Domokos. Dicke-model phase transition in the quantum motion of a bose-einstein condensate in an optical cavity. *Phys. Rev. Lett.*, 104(13):130401, Apr 2010.

[8] G. Szirmai, D. Nagy, and P. Domokos. Quantum noise of a bose-einstein condensate in an optical cavity, correlations, and entanglement. *Phys. Rev. A*, 81(4):043639, Apr 2010.

7 Zusammenfassung

Diese Bachelorarbeit beschäftigt sich mit ultra kalten Gasen in einem optischen Resonator. Wird das Bose-Einstein Kondensat (BEC) von einem Laser senkrecht zur Kavität angeregt, so ist es möglich, dass das Ensemble der sehr kalten Atome einen Phasenübergang vollzieht.
Das zunächst als homogene Wolke befindliche Kondensat bleibt wegen thermischer Fluktuationen stabil. In diesem Moment existiert kein Photon in der Kavität. Wird der Laser in seiner Intensität hochgefahren, gibt es einen Punkt, ab dem Photonen in die Kavität gestreut werden. Das Lichfeld in dem Resonator ermöglicht dem Bose-Einstein Kondensat einen energetisch günstigeren Zustand einzunehmen und sich selbst zu organisieren. Das sehr kalte Gas vollzieht also einen Phasenübergang und bildet eine Gitterstruktur innerhalb des Resonators.
Dieser Phasenübergang wurde erstmals von R.H. Dicke vorhergesagt [3] und ist auch als "Dicke Model Phase Transition" bekannt.
Das Dicke Model betrachtet das Kondensat als zwei Niveau System, wohingegen in dieser Arbeit das BEC als N-Level System behandelt wird. Dafür wird ein vollständiger Zustandsraum durch Bloch-Funktionen aufgespannt. Eine generalisierte Holstein-Primakoff Transformation, Verschiebeoperatoren und ein thermodynamischer Limes ermöglichen es den Hamiltonian als versetzten harmonischen Oszillator zu behandeln und ein effektives Model zu berechnen.
Es wird gezeigt, dass der Phasenübergang in Abhängigkeit der Intensität des Laser's in einem multi-Level System vollzogen wird. Dazu zeigt das exakte Model der normalen Phase, den Dicke-typischen verlauf des Übergangs. Ebenfalls werden die Besetzungswahrscheinlichkeiten der jeweiligen Moden in der super-radianten Phase numerisch berechnet. Die Ergebnisse signalisieren, dass eine multi-Level Betrachtung bei höheren Laserintensitäten wichtig ist.
Das hier vorgestellte multi-Level Dicke Model weist geringe Abweichnungen gegenüber der *mean field* Theorie [6] auf. Die Unterschiede können einerseits durch verschiedene numerische Verfahren begründet werden, andererseits durch den Unterschied der Methoden.